Development of a Reconstructed Cornea from Collagen–Chondroitin Sulfate Foams and Human Cell Cultures

N. Engin Vrana,[1] Nicolas Builles,[2] Virginie Justin,[2] Jurgen Bednarz,[3] Graziella Pellegrini,[4,5] Barbara Ferrari,[4] Odile Damour,[2,6] David J. S. Hulmes,[6] and Vasif Hasirci[1]

Purpose. To develop an artificial cornea, the ability to coculture the different cell types present in the cornea is essential. Here the goal was to develop a full-thickness artificial cornea using an optimized collagen–chondroitin sulfate foam, with a thickness close to that of human cornea, by coculturing human corneal epithelial and stromal cells and transfected human endothelial cells.

Methods. Corneal extracellular matrix was simulated by a porous collagen/glycosaminoglycan-based scaffold seeded with stromal keratocytes and then, successively, epithelial and endothelial cells. Scaffolds were characterized for bulk porosity and pore size distribution. The performance of the three-dimensional construct was studied by histology, immunofluorescence, and immunohistochemistry.

Results. The scaffold had 85% porosity and an average pore size of 62.1 μm. Keratocytes populated the scaffold and produced a newly synthesized extracellular matrix as characterized by immunohistochemistry. Even though the keratocytes lost their CD34 phenotype marker, the absence of smooth muscle actin fibers showed that these cells had not differentiated into myofibroblasts. The epithelial cells formed a stratified epithelium and began basement membrane deposition. An endothelial cell monolayer beneath the foam was also apparent.

Conclusions. These results demonstrate that collagen–chondroitin sulfate scaffolds are good substrates for artificial cornea construction with good resilience, long-term culture capability, and handling properties. (*Invest Ophthalmol Vis Sci.* 2008;49:5325–5331) DOI:10.1167/iovs.07-1599

From the [1]METU, BIOMAT, Department of Biological Sciences, Biotechnology Research Unit, Ankara, Turkey; [2]Banque de Cornées des Hospices Civils de Lyon, Lyon, France; [3]Kopf- und Hautzentrum, Klinik und Poliklinik für Augenheilkunde, Leiter der Hornhautbank, Hamburg, Germany; [4]The Veneto Eye Bank Foundation, Ospedale Civile di Venezia, Venice, Italy; and [6]Institut de Biologie et Chimie des Protéines, CNRS/Université de Lyon, Lyon, France.

[5]Present affiliation: Center for Regenerative Medicine "S. Ferrari," University of Modena and Reggio Emilio, 41100, Modena, Italy.

Supported by METU BAP, TUBITAK Grants TBAG 105T508 (NEV), the Hospices Civils de Lyon, the CNRS, the University of Lyon, and the European Union FP6 STREP project "Cornea Engineering" (contract NMP2-CT-2003-50417).

Submitted for publication December 24, 2007; revised May 20 and June 30, 2008; accepted October 9, 2008.

Disclosure: **N.E. Vrana**, None; **N. Builles**, None; **V. Justin**, None; **J. Bednarz**, None; **G. Pellegrini**, None; **B. Ferrari**, None; **O. Damour**, None; **D.J.S. Hulmes**, None; **V. Hasirci**, None

The publication costs of this article were defrayed in part by page charge payment. This article must therefore be marked "*advertisement*" in accordance with 18 U.S.C. §1734 solely to indicate this fact.

Corresponding author: Vasif Hasirci, METU, BIOMAT, Department of Biological Sciences, Biotechnology Research Unit, Ankara 06531, Turkey; vhasirci@metu.edu.tr.

Because of the limitations of artificial keratoprostheses, the shortage of donor corneas, and the risks of disease transmission or rejection after keratoplasty, there is a need to develop tissue-engineered corneas for corneal replacement and repair.[1] In addition, recent European directives have prohibited the use of laboratory animals in toxicity testing, particularly the use of the Draize eye irritancy test performed on rabbits.[2] There is, therefore, also a need for artificial corneal constructs that can replace animal models in pharmacotoxicology testing.

The cornea is composed of three distinct layers, each consisting of a different cell type. The corneal epithelium is the outermost layer and is composed of stratified squamous epithelial cells.[3] The epithelium is responsible for protection of the eye from physical agents. It also provides a smooth surface that facilitates oxygen and nutrient transport to the deeper layers of the cornea. The corneal stroma is the thickest layer (approximately 500 μm) and is composed of approximately 200 lamellae, in each of which the collagen fibrils are parallel to each other and of small, uniform diameter, essential for transparency.[4] Between neighboring lamellae, there is a sharp change in orientation, giving the overall structure a plywood-like organization essential for biomechanical properties. The stroma is populated by quiescent keratocytes.[5] Finally, the endothelial cell layer, by acting as a compensating pump,[6] is responsible for the liquid balance within the cornea that is critical for corneal opacity. Thus, to obtain a corneal equivalent, all three layers of the cornea must be present.

Collagens, as structural proteins, have attracted considerable interest as possible materials for building tissue-engineering scaffolds.[7] As natural polymers, they promote cell adhesion and proliferation better than synthetic polymers. They have been used successfully in a wide variety of tissue-engineering applications, such as skin, cartilage, bone, and nerve tissue engineering, alone or in combination with glycosaminoglycan (GAG) molecules.[8–12] Chondroitin sulfate is one of the most abundant GAGs in the human body and is generally present in the ECM (in the form of proteoglycans), together with collagens. Several studies have used the incorporation of chondroitin sulfate into collagenous matrices to better mimic the natural ECM and to increase functionality and mechanical properties.[8,9] This has been achieved through different methods, such as mixing collagen and chondroitin sulfate solutions with chitosan[13] and subsequently cross-linking the entire structure[14] or by adding chondroitin sulfate to the cross-linking solution during stabilization of the collagenous matrix.[15] Cross-linking can be achieved by chemical or physical means, such as dehydrothermal treatment or glutaraldehyde cross-linking. One of the most widely used cross-linking systems for collagen-based scaffolds is N-ethyl-N′-[3-dimethylaminopropyl]carbodiimide (EDC), N-hydroxy succinimide (NHS) cross-linking. This works through a mechanism in which EDC reacts with carboxyl groups to form a cross-link with amine groups. Use of NHS stabilizes the reaction by providing a more stable intermediate. This is a nontoxic, chemical cross-linking method

Copyright © Association for Research in Vision and Ophthalmology

Downloaded from iovs.arvojournals.org on 07/24/2020

TABLE 1. Primary Antibodies Used for Immunohistochemistry and Immunofluorescence

Antibody	Company	Specie	Reference	Dilution	Method
Collagen I	Novotec	Rabbit	20111	1/500	Immunohistochemistry
Collagen V	Novotec	Rabbit	20511	1/100	Immunohistochemistry
Collagen VI	Novocastra	Mouse	Ncl-collVI	1/25	Immunohistochemistry
CD34	TEBU BIO	Mouse	038NCLEND	1/100	Immunohistochemistry
α-SMA	TEBU BIO	Mouse	038NCLSMA	1/100	Immunohistochemistry
Nestin	R&D Systems	Mouse	MAB1259	1/100	Immunohistochemistry
Vimentin	R&D Systems	Mouse	MAB2105	1/100	Immunohistochemistry
Collagen IV	Novocastra	Mouse	NCL-COLL-IV	1/30	Immunofluorescence (FITC)
Keratin 3	Progen	Mouse	61807	1/100	Immunofluorescence (FITC)
SV40 large T antigen	PharMingen	Mouse	554149	1/100	Immunofluorescence (Alexa Fluor 488)

that has been shown to be beneficial for cell viability and stability.[16,17]

Transplantable epithelial[18] and endothelial[19] cell sheets have been reported for the reconstruction of human cornea cell layers. For the reconstruction of multiple cell layers, either corneal stromas have been reconstituted as collagen gels containing corneal keratocytes or cells have been seeded into prefabricated foams or sponges; both have then been used as supports for epithelial or endothelial cell layers.[20,21] Griffith et al.[22] reconstituted glutaraldehyde cross-linked collagen–chondroitin sulfate gels mixed with human keratocytes to which epithelial and endothelial cell layers were added—all with immortalized human cells—for use in drug and toxicity testing. In an alternative approach, prefabricated collagen-based sponges cross-linked by dehydrothermal treatment were used to investigate the behavior of normal human keratocytes, epithelial cells, and endothelial cells, separately and in coculture, and were found to influence cell proliferation, cell morphology, and ECM synthesis.[23] Such an approach has been used more recently[13] with collagen–chondroitin sulfate–chitosan sponges to reconstruct human hemicorneas (stroma and epithelium) using normal human keratocytes and limbal stem cell–derived epithelial cells for pharmacotoxicity testing. Collagen films have also been investigated as scaffolds for stromal reconstruction,[24–26] as have synthetic polymer–based scaffolds, either alone[27,28] or in combination with collagen.[29]

An EDC/NHS cross-linked collagen hydrogel has recently been used in a corneal implant animal model.[30] Here we describe the development of an EDC/NHS cross-linked collagen–chondroitin sulfate scaffold to reconstruct full-depth corneas in vitro using normal human keratocytes, adult limbal stem cell–derived human epithelial cells, and transformed human endothelial cells. The distribution and localization of the different cell types were investigated, as were their state of differentiation and the deposition of new ECM components.

MATERIALS AND METHODS

Materials

Rat tail type I collagen (purity 99%) and 70-μm cell sieves were purchased from BD Biosciences (Franklin Lakes, NJ). Chondroitin sulfate A from bovine trachea, EDC, NHS, trypsin-EDTA, and Evans Blue were purchased from Sigma-Aldrich (Seelze, Germany). Acetic acid, sodium dihydrogen phosphate, and disodium hydrogen phosphate were obtained from Merck (Darmstadt, Germany). Diaminobenzidine (DAB) enzyme substrate was purchased from Dako (Ulis, France), Hoechst 33258 was obtained from TEBU-Bio (Le Perray en Yvelines, France), and collagenase A from *Clostridium histolyticum* was bought from Roche (Indianapolis, IN). Full details of the primary antibodies used in immunostaining experiments are given in Table 1. Secondary antibodies used in immunostaining were FITC-conjugated sheep anti–mouse IgG and Alexa Fluor 488 goat anti–mouse IgG, which were purchased from Cedarlane (Burlington, ON, Canada), TEBU-Bio, and Invitrogen (Carlsbad, CA), respectively.

Scaffold Preparation

Rat tail collagen solution (750 μL, 3 mg/mL in 0.02% acetic acid) was poured into plastic tissue culture plates (diameter, 1.6 cm), and EDC/NHS solution (100 μL in 50 mM NaH_2PO_4 [pH 5.5] buffer) was added to each plate to reach a final wt/wt ratio of 1.00/1.13/1.00 of collagen/EDC/NHS. After vigorous mixing, the final solution was incubated for 2 hours at room temperature and, after cross-linking, was lyophilized for 8 hours. Resultant foams were immersed in a 3 mg/mL chondroitin sulfate solution and then air dried. Subsequently, for cross-linking of the absorbed chondroitin sulfate, the construct was immersed in EDC/NHS solution (33 mM and 6 mM, respectively, in 50 mM NaH_2PO_4 buffer [pH 5.5]) for 1 hour at 4°C, followed by incubation in 0.1 M Na_2HPO_4 buffer (pH 9.1) for 1 hour to stabilize the pH, then washing in 2 M and 1 M NaCl solution. Constructs were lyophilized and stored in a desiccator at room temperature.

Scaffold Characterization

Foam Thickness Measurement. Foam thicknesses were measured using a standard micrometer with a sensitivity of 0.1 μm for cross-linked collagen and collagen–chondroitin sulfate foams. Each sample was measured at least three times, and six samples each were used for both cross-linked and non–cross-linked specimens.

Bulk Porosity of Foams. Bulk porosity of the cross-linked collagen and the collagen–chondroitin sulfate foams was determined ($n \geq 6$) using a helium pycnometer (Ultrapycnometer 1000; Quantachrome, Boynton Beach, FL). The volume of the foam filled by helium (V_{He}) was measured, and the bulk porosity (%) was calculated using the following formula, where the initial volume of the foam (V_f) was calculated from its known dimensions:

$$\frac{V_{He}}{V_f} \times 100 = \text{Porosity (\%)}$$

Pore Size Distribution. The pore size distributions for the non–cross-linked and cross-linked collagen and for the cross-linked collagen–chondroitin sulfate foams ($n \geq 6$) were determined with the use of a mercury porosimeter (Poremaster 60; Quantachrome) under low pressure (50 psi).

In Vitro Studies

Origin, Isolation, and Culture of Keratocytes. Keratocytes were isolated from excised human corneas in accordance with ethical regulations (Bioethics Law no. 2004-800; France). The corneas selected were unusable for treatment because of their low endothelial cell density and were stored at 31°C in organ culture. Cell isolation was performed by incubating the corneas in a 3-mg/mL collagenase A

Downloaded from iovs.arvojournals.org on 07/24/2020

solution for 3 hours at 31°C while stirring at 200 rpm. The digest was purified through a 70-μm cell sieve and was immediately placed in monolayer culture.

Keratocytes were seeded at a density of 10,000 cells/cm^2 and were cultured in a specially designed medium providing optimal growth and preservation of the phenotype.[31] The composition of the medium was as follows: DMEM/Ham-F12 1:1, 10% newborn calf serum, 5 ng/mL basic fibroblast growth factor, and antibiotics (penicillin, gentamicin, B-amphotericin). The medium was changed every 2 days until cell confluence was attained. At confluence, cells were resuspended using trypsin-EDTA (0.5 g trypsin/L and 0.2 g EDTA/L), amplified over 1 passage (P0), and seeded at P1 inside the matrix.

Origin and Culture of Epithelial Cells. Limbal stem cells were isolated from human corneas in accordance with the tenets of the Declaration of Helsinki (The Veneto Eye Bank Foundation, Venice, Italy). Corneas were taken (after permission) from organ donors and examined with a slit lamp immediately after retrieval; those not suitable for transplantation were used for cell isolation. Briefly, samples were treated with 0.05% trypsin and 0.01% EDTA for approximately 80 minutes Cells were collected every 20 minutes, plated at a density of 1.5×10^4 cells/cm^2 on lethally irradiated 3T3-J2 cells (2.4×10^4 cells/cm^2), and incubated at 37°C and 5% CO_2, as previously described.[32]

Colony-forming efficiency assays and calculation of the number of cell generations were performed as described.[32] Briefly, 300 to 2000 cells from each sample were plated onto 3T3 feeder layers. Colonies were fixed 12 days later, stained with rhodamine B, and scored under a dissecting microscope. Cells at passage 2 were seeded on foams at a density of 2.5×10^5 cells/cm^2.

Origin and Culture of Endothelial Cells. SV40-transfected human endothelial cells were isolated and cultured according to a protocol established earlier.[33] They were used at passage 66, at 2×10^6 cells per matrix, taking into consideration cell loss during seeding.

Preparation of Reconstructed Cornea. The diameter of each collagen–chondroitin sulfate foam was 1.2 cm (4.5 cm^2 surface area), and the starting thickness was 500 μm. Ten collagen–chondroitin sulfate foams were seeded with 5×10^5 keratocytes (passage 1) in keratocyte medium. At day 18, a single sample was tested for keratocyte penetration. After 49 days of keratocyte culture, epithelial cells were seeded on top of these foams at a density of 2.5×10^5cells/cm^2. At 56 days, the construct was placed at the air-liquid interface to induce differentiation of the epithelial layers. At day 71, four hemicorneas were used for evaluation, leaving five hemicorneas for the remainder of the experiment. On day 81 of culture, the five remaining hemicorneas were endothelialized with 2×10^6 SV40 endothelial cells, giving rise to the reconstructed full-thickness corneas. At 84 days, the culture was stopped and the corneas were characterized, as described. On the whole, the culture time was 84 days for keratocytes, 35 days for epithelial cells, and 3 days for SV40 endothelial cells.

Histology. Tissue equivalents were fixed with 10% formalin solution and embedded in paraffin. Six-micrometer–thick sections were cut and stained using hematoxylin-phloxin-saffron.

Immunofluorescence. Tissue equivalents were embedded in OCT compound (Tissue-Tek; Qiagen, Valencia, CA) and frozen. Frozen sections (6 μm) were blocked in phosphate-buffered saline containing 1% (wt/vol) bovine serum albumin. Immunofluorescence studies were performed with monoclonal and polyclonal antibodies for cytokeratin 3, collagen IV, and SV40 large T antigen (Table 1). The secondary antibody was FITC-conjugated sheep anti–mouse IgG (1/100 dilution) or Alexa Fluor 488–conjugated goat anti–mouse IgG (1/100 dilution). The secondary antibody was mixed with Hoechst 33258 (1/100 dilution) to stain the nuclei and 0.1% Evans Blue to reduce the nonspecific staining of the biopolymer network. The primary antibody was replaced by an IgG isotype in negative controls. Positives controls on human skin were made for collagen IV.

Immunohistochemistry. Reconstructed corneas were fixed in 10% formaldehyde and embedded in paraffin. Five-micrometer sections were cut and incubated with primary antibodies, followed by secondary antibodies coupled to peroxidase. A brown precipitate indicating the distribution of the target protein became visible on the addition of a diaminobenzidine enzyme substrate. Primary antibodies against human collagen types I, V, and VI, CD34, α-SMA, nestin, and vimentin were used (Table 1). Unmasking techniques were performed for collagen types I and V with hyaluronidase and for type VI collagen with boiling citrate and trypsin treatment. There was no cross-reactivity between the anti–collagen antibodies used and the collagen in the foam (made using rat tail tendon collagen). The primary antibody was replaced by an IgG isotype in negative controls. Positive controls on human skin were made.

TABLE 2. Characteristics of Foam Types

Foam Type	Thickness (μm)	Porosity (%)	Pore Size (μm)
Non–cross-linked collagen	721 ± 17.6	—	63.8
Cross-linked collagen	531.6 ± 23.7	95.8	35.6
Cross-linked collagen-chondroitin sulfate	678.3 ± 30.6	85.00	62.1

RESULTS

Scaffold Characterization

Cross-linking of preassembled rat tail collagen foams caused extreme shrinkage of the foam. To prevent this, the cross-linking step was carried out by EDC/NHS within the collagen solution before lyophilization and foam formation. In this way foams preserved a significant (74.6%) level of their original thickness. Their final thickness was 531.6 ± 23.7 μm. Without this cross-linkage in solution, foams preserved only 10% of their initial thickness.

Incorporation of chondroitin sulfate into the foam structure caused some structural changes in final thickness, overall porosity, and average pore size. The thickness of the foams increased to 678.3 ± 30.6 μm ($P \leq 0.001$). Cross-linked pure collagen foams had a porosity of 95.8% (vol/vol). After the addition of chondroitin sulfate, porosity decreased to 85.0% (vol/vol). Mercury porosimetry showed that collagen–chondroitin sulfate foams had an average pore size of 62.1 μm, a value higher than that of the collagen foams (35.6 μm; Table 2).

Histology

Figure 1 shows the whole construct. In the central stromal-like region, keratocytes were distributed uniformly throughout the foam, demonstrating that these cells had migrated deeply into the scaffold. On the upper surface, the epithelial layer appeared as a thin, differentiated, stratified epithelium. On the lower surface, the endothelial monolayer was clearly visible as a line of cells resting on a layer of dense keratocytes and neosynthesized matrix that served as an anchoring support. In contrast, neither Bowman membrane nor Descemet membrane, two structures easily viewed, when present, by optical microscopy as thick collagenous layers, was observed.

Immunofluorescence and Immunohistochemistry

Immunofluorescence and immunohistochemistry were carried out to assess the nature, extent, and localization of the newly synthesized ECM secreted by the keratocytes, the formation of a basal lamina by the epithelial cells, and the phenotype of the different cell types.

Differentiated epithelial cells showed the classical cytokeratin 3 staining for corneal epithelium (Fig. 2a). Basal lamina deposition was shown by the collagen type IV–positive staining between the epithelial and stromal layers (Fig. 2b). SV40 labeling revealed the endothelial cell monolayer on the lower

Downloaded from iovs.arvojournals.org on 07/24/2020

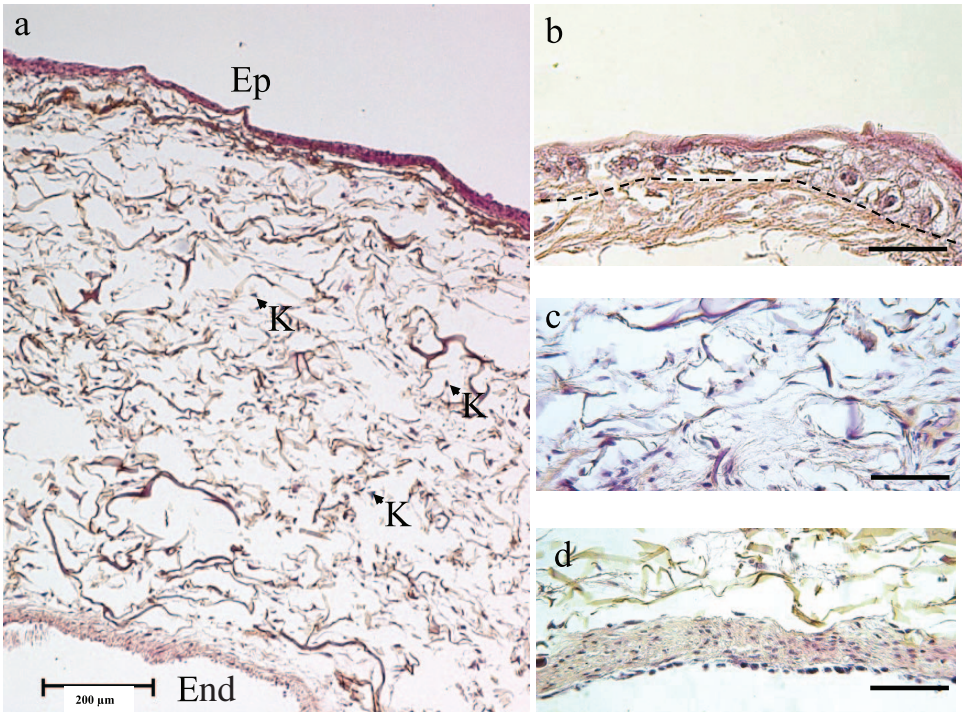


FIGURE 1. Histology of the construct at day 84. (**a**) General view of the construct: epithelium (Ep), keratocytes (K) deep inside the stromal construct, endothelial layer (End). (**b**) Epithelium. (**c**) Stroma. (**d**) Endothelial layer. All staining: Hematoxylin-phloxin-saffron. Scale bar: (**a**) 200 μm; (**b**) 50 μm; (**c, d**) 100 μm.

surface of the construct (Fig. 2c). Not all transfected endothelial cells stained for SV40 antigen, but this is to be expected because the expression of large T antigen fades with successive population doublings. Proliferation of these endothelial cells on the foam surface stopped with contact inhibition.

To determine the secretion of newly synthesized ECM by keratocytes, constructs were stained for collagen types I, V, and VI. Collagen type I staining was found throughout the foam, along with the keratocytes (Fig. 3a). Collagen V could also be detected inside the foam but had a preferential subepithelial localization (Fig. 3c). Collagen VI was localized around the keratocytes (Fig. 3d). The harsh boiling citrate treatment used for collagen VI destroyed most of the epithelial layer, leaving only basal cells (Fig. 3d).

Few keratocytes stained for CD34 antigen, and none stained for α-SMA (Figs. 4a, 4b). However, they did express nestin and the associated intermediary filament protein vimentin (Figs 4c, 4d).

DISCUSSION

The human cornea is approximately 500 μm thick, and foams should have a thickness close to this value. With the use of appropriate molds and lyophilization conditions, this can be achieved. Cross-linking of rat tail collagen foams with conventional methods (immersion of the scaffold into the cross-linking medium), however, led to extreme shrinkage and loss of the porous structure. This was prevented by introduction of the

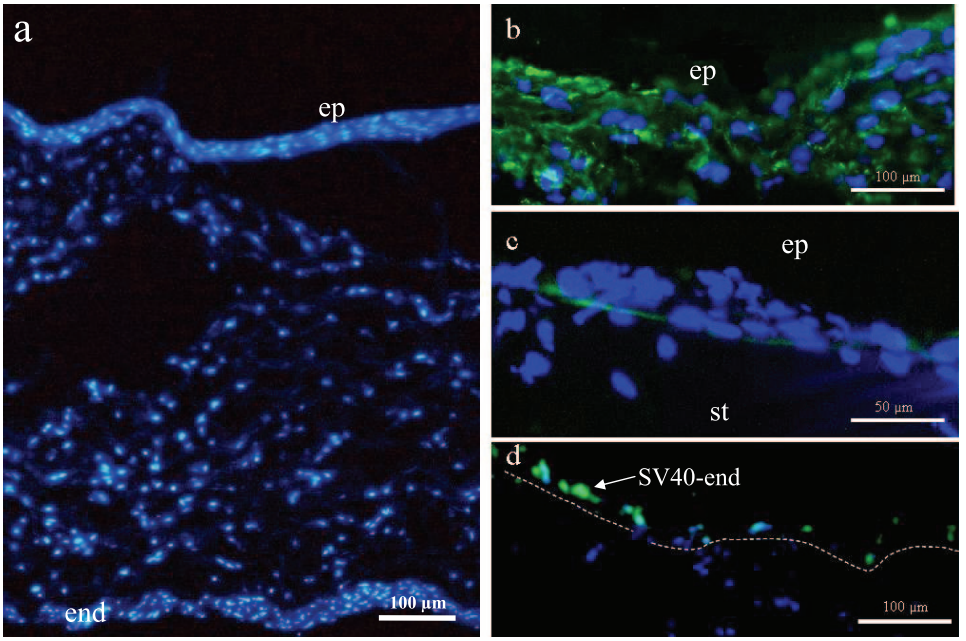


FIGURE 2. Immunofluorescence. (**a**) Hoechst staining of cell nuclei showing the distribution of cells inside the matrix. Hoechst 33258 (1/100 dilution). (**b**) Epithelium, cytokeratin 3, immunofluorescence (*green*, keratin 3; *blue*, nuclei). (**c**) Basal lamina, epithelial side, stromal side, collagen IV, immunofluorescence. (**d**) Endothelium SV40 antigen, immunofluorescence (SV40-end) endothelial cell SV40 stained (*green*, SV40 large T antigen; *blue*, nuclei; *dotted line*, scaffold limits). ep, epithelial side; end, endothelial side; st, stromal side. Scale bar: (**a**, **b**) 100 μm; (**c**, **d**) 50 μm.

Downloaded from iovs.arvojournals.org on 07/24/2020

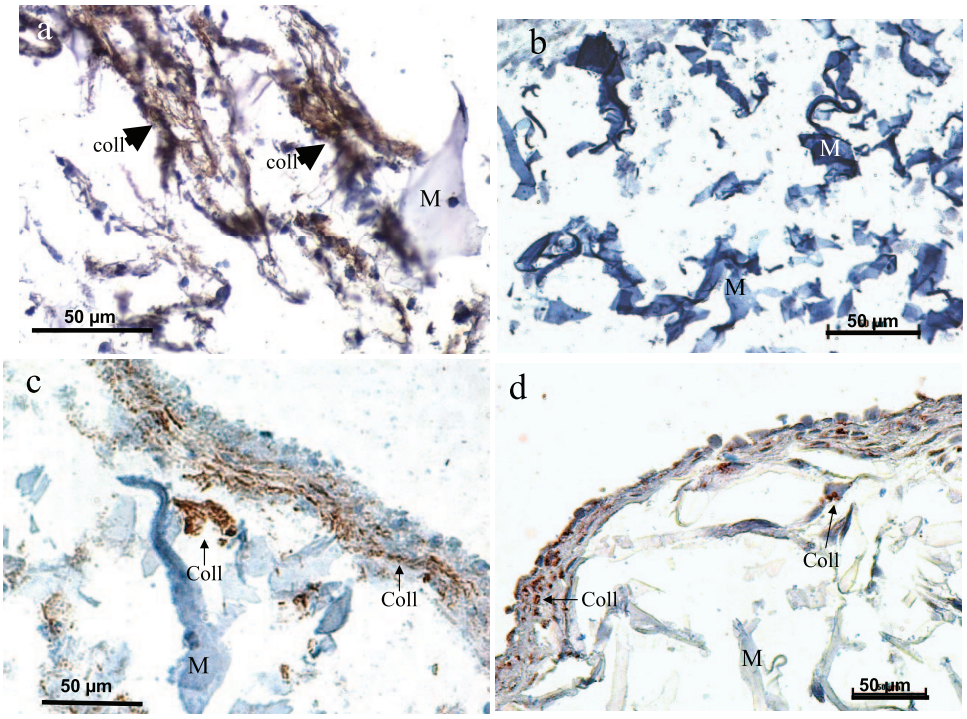


FIGURE 3. Immunohistochemistry of newly synthesized collagens in a 71-day construct. (**a**) Collagen type I human (*tan*) in the collagen-chondroitin sulfate foam (*blue*). (**b**) Negative control for collagen type I. (**c**) Newly synthesized collagen type V (*tan*) preferentially localized at the surface of the stromal layer. (**d**) Newly synthesized collagen type VI (*tan*). coll, newly synthesized collagen; M, initial matrix. Scale bar, 50 μm.

cross-linker couple before lyophilization (i.e., before the formation of foam), which resulted in a smaller change in the physical properties of the foam, such as thickness and porosity. The second cross-linking step for stabilization of chondroitin sulfate within the foam body also affected the three-dimensional structure of the collagen fibrils, leading to a decrease in porosity, probably as a result of the additional cross-linking. In contrast, average pore size increased after the introduction of chondroitin sulfate, perhaps because of selective cross-linking of small-diameter pores. In any case, porosity and pore size were well within the optimal range.[34,35]

Coculturing of the epithelial and stromal layers was successful and resulted in a multilayered epithelium and a populated stroma. At the end of the culture, the final thickness was more than the initial thickness of the foam because of epithelial cell growth, keratocyte invasion, and stromal hydration, consistent with our previous observations with collagen scaffolds seeded with keratocytes.[36] Further addition of endothelial cells provided the system with an endothelial lining. Thus, the proposed model successfully mimicked the three layers of the native cornea. Moreover, the presence of an endothelial cell layer should prevent the overhydration of the construct by regulating water content. However, it

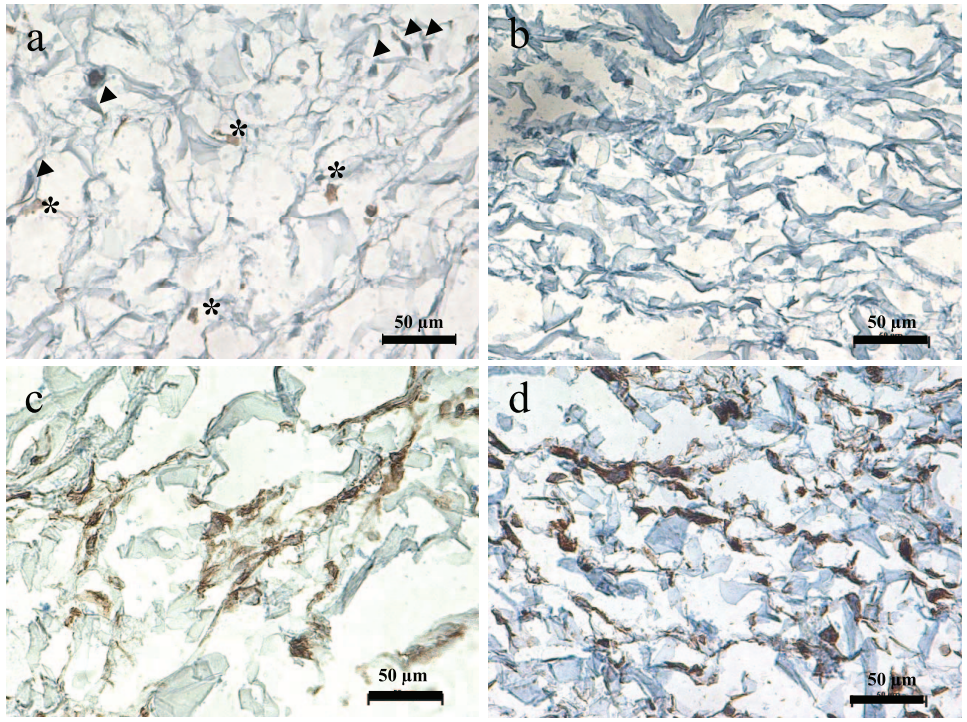


FIGURE 4. Characterization of keratocytes by immunohistochemistry. (**a**) CD34 staining. Cell bodies without CD34 (*arrows*) are mixed with $CD34^+$ cells body (*asterisk*). (**b**) α-SMA staining. All cells are negative for α-SMA. (**c**) Vimentin staining: all cells are positive for vimentin. (**d**) Nestin staining: all cells are positive. Scale bar, 50 μm.

Downloaded from iovs.arvojournals.org on 07/24/2020

lacked both the Bowman and the Descemet membranes. The absence of the Descemet membrane could be attributed to the short culture time of the endothelial cells in the system (3 days), which are responsible for the secretion of this layer.[37] Moreover, SV40 transfection and subsequent culturing may affect the endothelial cell phenotype, which can affect basement membrane secretion. Finally, the surface provided by the foam is relatively porous and rough, which may also affect endothelial cell secretion. The foam had a surface skin layer that acted as an initial basement membrane for epithelial cells on the top surface. This layer can become more porous during keratocyte culture within the foams, thus providing epithelial cells with a more porous three-dimensional environment that would alter epithelial cell behavior and epithelial-keratocyte interactions and thus prolonging the secretion of a well-defined Bowman membrane.[38] The presence of layers of corneal keratocytes close to both the bottom and the top surface of the scaffolds indicates that the culture system will have distinct layers after remodeling.

Stromal keratocytes are quiescent cells responsible for the remodeling of the stromal ECM. Our immunohistochemistry results showed that keratocytes secreted ECM molecules such as collagen types I, V, and VI, known to be particularly abundant in the corneal stroma.[5] This significant ECM secretion by keratocytes begins to fill the porous structure of the scaffold. The qualitative distribution of the main components of the newly secreted ECM was close to that in the normal human cornea.[5] Moreover, the preferential localization of collagen type V at the interface of the epithelial and stromal layers is indicative of dynamic epithelium-keratocyte interactions in the construct, which would increase the similarity of the model to in vivo conditions.[39]

On injury, keratocytes generally are converted to a more fibroblastic phenotype, increasing their proliferation and secretion to overcome the damage incurred.[40] This conversion can be followed by the loss of the stellar appearance of the keratocytes and the acquisition of a more spindle-like morphology. This keratocyte-myofibroblast conversion can be monitored by using myofibroblast- or keratocyte-specific markers. The CD34 surface antigen has been shown to be a specific marker of the keratocyte phenotype, whereas the appearance of α-SMA fibers is an indicator of myofibroblastic conversion.[41,42]

Previous studies by the authors have shown that neosynthesized collagen deposition in collagen foams is a slow process. An initial study[13] showed that 35-day culture provides incomplete filling of the pores of the foam. In another study,[43] we tried to increase collagen deposition and to observe the effect of tetracycline hydrochloride treatment on a 74-day culture with some success. This explains the long time in culture for the keratocytes. In the same study, we demonstrated the influence of epithelial-keratocyte interactions on the quality of the reconstructed stroma. This resulted in a long coculture time, 25 days, for our epithelialized foam because we wanted to be as close as possible to a "normal human cornea."

The stroma of the corneal construct was populated with keratocytes from the cornea of a human donor. These keratocytes were passaged only once on plastic (to generate a sufficient number of cells). Despite this short time in monolayer culture in a specially optimized culture medium, most lost their CD34 expression and shifted to a more fibroblastic phenotype. Parallel observations on cells seeded on slides showed that only approximately 33% expressed CD34 (data not shown). Given that CD34 appears to have a role in cell-matrix adhesion with a selectin-like ligand in native cornea, it is possible that keratocytes must avoid attachment to spread inside the foam and to synthesize new ECM. This would explain the loss of CD34 antigen expression. On the other hand, the absence of α-SMA expression shows that the cells did not acquire a myofibroblast phenotype. We also demonstrated the neural crest origin of the keratocytes used in our model by their expression of nestin and the associated intermediary filament protein vimentin,[44] as in the native cornea. Taken together, these results suggest that in this three-dimensional model, the keratocytes either kept their phenotype, but with decreased CD34 antigen expression, or they changed to a fibroblastic phenotype. The phenotype was close enough to the keratocyte phenotype to synthesize normal corneal ECM with respect to collagen deposition. The present stromal model is in a dynamic stage of ECM formation, unlike the normal adult human cornea, which may result in a different expression profile for the keratocytes. Initially, constructs were not transparent, and the increase in transparency during the initial stages of culture with keratocytes, as observed by the ability to read a printed letter with 14-point Arial font, was slow. The structure became translucent in the later stages of the culture primarily because of degradation and remodeling of the scaffold by keratocytes, as shown by the collagen secretion. Lack of evidence on myofibroblast differentiation suggested the secretion would not lead to scar formation.

A cell monolayer at the bottom of the foams was achieved when endothelial cells were added to the construct. Even though these SV40-transformed cells are suitable for pharmacotoxicologic purposes[45] despite their human origin, they are not representative of the normal corneal endothelium. The current model proposed is suitable for pharmacotoxicologic testing because it supported long-term coculture of all three corneal cell types in a three-dimensional culture system. This is useful because the effects of administered drugs can be determined not only by cell proliferation and apoptosis, as in a two-dimensional culture system, but also by cell distribution and secretion, as in a three-dimensional culture system.[46] The next step in the assessment of this model will be to compare it with an in vivo animal model, with well-known toxic agents, to more comprehensively evaluate its functionality in pharmacotoxicologic applications. Human endothelial cells will also be used to more closely mimic the in vivo situation.

Conclusions

These results demonstrate that collagen–chondroitin sulfate scaffolds are good substrates for artificial cornea construction. This model has the following interesting properties: it is capable of sustaining long-term culture, it is resilient, and its handling properties make it suitable for pharmacotoxicologic and drug safety testing. With the incorporation of nontransformed human endothelial cells, this system could be developed as a full-thickness human artificial cornea, constituting a step toward a substitute for corneal transplantation.

Acknowledgments

Mercury porosimetry and helium pycnometry were performed at the METU Central Laboratory.

References

1. Duan D, Klenkler BJ, Sheardown H. *Expert Rev Med Devices.* 2006;3(1):59–72.
2. Wilhelmus KR. The Draize eye test. *Surv Ophthalmol.* 2001;45(6):493–515.
3. Beuerman RW, Pedroza L. Ultrastructure of the human cornea. *Microscopy Res Technique.* 1996;33(4):320–325.
4. Meek KM, Boote C. The organization of collagen in the corneal stroma. *Exp Eye Res.* 2004;78(3):503–512.
5. Robert L, Legais JM, Robert AM, Renard G. Corneal collagens. *Pathol Biol.* 2001;49(4):353–363.
6. Bonanno JA. Identity and regulation of ion transport mechanisms in the corneal endothelium. *Progress Retinal Eye Res.* 2003;22(1):69–94.
7. Lee CH, Singla A, Lee Y. Biomedical applications of collagen. *Int J Pharm.* 2001: 22(23):3145–3154.

Downloaded from iovs.arvojournals.org on 07/24/2020

8. Black AF, Bouez C, Perrier E, et al. Optimization and characterization of an engineered human skin equivalent. *Tissue Eng.* 2005; 11(5):723–733.
9. Augustin C, Collombel C, Damour O. Use of in vitro dermal equivalent and skin equivalent kits for evaluating cutaneous toxicity of cosmetics products. *In Vitro Toxicol.* 1997;10(1):23–31.
10. Lee CR, Grodzinsky AJ, Spector M. The effects of cross-linking of collagen-glycosaminoglycan scaffolds on compressive stiffness, chondrocyte-mediated contraction, proliferation and biosynthesis. *Biomaterials.* 2001;22(23):3145–3154.
11. Yaylaoglu MB, Yildiz C, Korkusuz F, Hasirci V. A novel osteochondral implant. *Biomaterials.* 1999;20(16):1513–1520.
12. Chamberlain LJ, Yannas IV, Hsu HP, Strichartz GR, Spector M. Near terminus axonal structure and function following rat sciatic nerve regeneration through a collagen-GAG matrix in a ten-millimeter gap. *J Neurosci Res.* 2000;60(5):666–677.
13. Builles N, Bechetoille N, Justin V, et al. Development of a hemicornea from human primary cell cultures for pharmacotoxicology testing. *Cell Biol Toxicol.* 2007;23(4):279–292.
14. Pek YS, Spector M, Yannas IV, Gibson LJ. Degradation of a collagen-chondroitin-6-sulfate matrix by collagenase and by chondroitinase. *Biomaterials.* 2004;25(3):473–482.
15. van Susante JLC, Piepe J, Buma P, et al. Linkage of chondroitin-sulfate to type I collagen scaffolds stimulates the bioactivity of seeded chondrocytes in vitro. *Biomaterials.* 2001;22(17):2359–2369.
16. Powell HM, Boyce ST. EDC cross-linking improves skin substitute strength and stability. *Biomaterials.* 2006;27(34):5821–5827.
17. Ber S, Köse GT, Hasirci V. Bone tissue engineering on patterned collagen films: an in vitro study. *Biomaterials.* 2005;26(14):1977–1986.
18. Rama P, Bonini S, Lambiase A. Autologous fibrin-cultured limbal stem cells permanently restore the corneal surface of patients with total limbal stem cell deficiency. *Transplantation.* 2001;72(9): 1478–1485.
19. Ide T, Nishida K, Yamato M, et al. Structural characterization of bioengineered human corneal endothelial cell sheets fabricated on temperature-responsive culture dishes. *Biomaterials.* 2006;27(4): 607–614.
20. Germain L, Auger FA, Grandbois E, et al. Reconstructed human cornea produced in vitro by tissue engineering. *Pathobiology.* 1999;67(3):140–147.
21. Orwin EJ, Hubel A. In vitro culture characteristics of corneal epithelial, endothelial, and keratocyte cells in a native collagen matrix. *Tissue Eng.* 2000;6(4):307–319.
22. Griffith M, Osborne R, Munger R, et al. Functional human corneal equivalents constructed from cell lines. *Science.* 1999;286(5447): 2169–2172.
23. Orwin EJ, Borene ML, Hubel A. Biomechanical and optical characteristics of a corneal stromal equivalent. *J Biomech Eng.* 2003; 125(4):439–444.
24. Torbet J, Malbouyres M, Builles N, et al. Orthogonal scaffold of magnetically aligned collagen lamellae for corneal stroma reconstruction. *Biomaterials.* 2007;28(29):4268–4276.
25. Vrana E, Builles N, Hindie M, Damour O, Aydinli A, Hasirci V. Contact guidance enhances the quality of a tissue engineered corneal stroma. *J Biomed Mater Res A.* 2008;84(2):454–463.
26. Vrana NE, Elsheikh A, Builles N, Damour O, Hasirci V. Effect of human corneal keratocytes and retinal pigment epithelial cells on the mechanical properties of micropatterned collagen films. *Biomaterials.* 2007;28(29):4303–4310.
27. Zorlutuna P, Tezcaner A, Kiyat I, Aydinli A, Hasirci V. Cornea engineering on polyester carriers. *J Biomed Mater Res A.* 2006; 79(1):104–113.
28. Zorlutuna P, Builles N, Damour O, Elsheikh A, Hasirci V. Influence of keratocytes and retinal pigment epithelial cells on the mechanical properties of polyester-based tissue engineering micropatterned films. *Biomaterials.* 2007;28(24):3489–3496.
29. Li F, Carlsson D, Lohmann C, et al. Cellular and nerve regeneration within a biosynthetic extracellular matrix for corneal transplantation. *Proc Natl Acad Sci U S A.* 2003;100(26):15346–15351.
30. Liu Y, Gan L, Carlsson DJ, et al. A simple, crosslinked collagen tissue substitute for corneal implantation. *Invest Ophthalmol Vis Sci.* 2006;47(5):1869–1875.
31. Builles N, Bechetoille N, Justin V, et al. Development of an optimised culture medium for keratocytes in monolayer Bio-Med. *Mat Eng.* 2006;16(suppl):S95–S104.
32. Pellegrini G, Golisano O, Paterna P, et al. Location and clonal analysis of stem cells and their differentiated progeny in the human ocular surface. *J Cell Biol.* 1999;145(4):769–782.
33. Bednarz J, Teifel M, Friedl P, Engelmann K. Immortalization of human corneal endothelial cells using electroporation protocol optimized for human corneal endothelial and human retinal pigment epithelial cells. *Acta Ophthalmol Scand.* 2000;78(2):130–136.
34. Barry JJA, Silva MMCG, Cartmell SH, Guldberg RE, Scotchford CA, Howdle SM. Porous methacrylate tissue engineering scaffolds: using carbon dioxide to control porosity and interconnectivity. *J Mater Sci.* 2006;41:4197–4204.
35. O'Brien FJ, Harley BA, Yannas IV, Gibson LJ. The effect of pore size on cell adhesion in collagen-GAG scaffolds. *Biomaterials.* 2005; 26(4):433–441.
36. Vrana NE, Builles N, Kocak H, et al. EDC/NHS crosslinked collagen foams as scaffolds for artificial corneal stroma. *J Biomater Sci Polym Ed.* 2007;18(12):1527–1545.
37. Nishimura T, Toda S, Mitsumoto T, Oono S, Sugihara H. Effects of hepatocyte growth factor, transforming growth factor-β1 and epidermal growth factor on bovine corneal epithelial cells under epithelial-keratocyte interaction in reconstruction culture. *Exp Eye Res.* 1998;66(1):105–116.
38. Wilson SE, Liu JJ, Mohan RR. Stromal-epithelial interactions in the cornea. *Prog Retin Eye Res.* 1999;18(3):293–309.
39. Leung EW, Rife E, Smith RE, Kay EP. Extracellular matrix components in retrocorneal fibrous membrane in comparison to corneal endothelium and Descemet's membrane. *Mol Vis.* 2000;7(6):15–23.
40. Wilson SE, Mohan RR, Mohan RR, et al. The corneal wound healing response: cytokine-mediated interaction of the epithelium, stroma, and inflammatory cells. *Prog Retin Eye Res.* 2001;20(5):625–637.
41. Toti P, Tosi GM, Traversi C, Schürfeld K, Cardone C, Caporossi A. CD-34 stromal expression pattern in normal and altered human corneas. *Ophthalmology.* 2002;109(6):1167–1171.
42. Jester JV, Huang J, Fisher S, et al. Myofibroblast differentiation of normal human keratocytes and hTERT, extended-life human corneal fibroblasts. *Invest Ophthalmol Vis Sci.* 2003;44(5):850–858.
43. Builles N, Justin V, André V, Burillon C, Damour O. Reconstructed corneas: effect of three-dimensional culture, epithelium, and tetracycline hydrochloride on newly synthesized extracellular matrix. *Cornea.* 2007;26(10):1239–1248.
44. Lwigale PY, Cressy PA, Bronner-Fraser M. Corneal keratocytes retain neural crest progenitor cell properties. *Dev Biol.* 2005; 288(1):284–293.
45. Reichl S, Bednarz J, Müller-Goymann CC. Human corneal equivalent as cell culture model for in vitro drug permeation studies. *Br J Ophthalmol.* 2004;88(4):560–565.
46. MacGregor JT, Collins JM, Sugiyama Y, et al. In-vitro human tissue models in risk assessment: report of a consensus-building workshop. *Toxicology.* 2001;(59):17–36.

Downloaded from iovs.arvojournals.org on 07/24/2020